Applied and Environmental Microbiology, May 2008, p. 2967–2975 Vol. 74, No. 10
0099-2240/08/$08.00+0 doi:10.1128/AEM.02768-07

Efficient Production of L-Ribose with a Recombinant *Escherichia coli* Biocatalyst▽

Ryan D. Woodyer,[1]* Nathan J. Wymer,[1]† F. Michael Racine,[1] Shama N. Khan,[1] and Badal C. Saha[2]

zuChem, Inc., 2225 W. Harrison, Suite F, Chicago, Illinois 60612,[1] and Fermentation Biotechnology Research Unit, National Center for Agricultural Utilization Research, Agricultural Research Service, U.S. Department of Agriculture, Peoria, Illinois 61604[2]

Received 7 December 2007/Accepted 8 March 2008

A new synthetic platform with potential for the production of several rare sugars, with L-ribose as the model target, is described. The gene encoding the unique NAD-dependent mannitol-1-dehydrogenase (MDH) from *Apium graveolens* (garden celery) was synthetically constructed for optimal expression in *Escherichia coli*. This MDH enzyme catalyzes the interconversion of several polyols and their L-sugar counterparts, including the conversion of ribitol to L-ribose. Expression of recombinant MDH in the active form was successfully achieved, and one-step purification was demonstrated. Using the created recombinant *E. coli* strain as a whole-cell catalyst, the synthetic utility was demonstrated for production of L-ribose, and the system was improved using shaken flask experiments. It was determined that addition of 50 to 500 μM $ZnCl_2$ and addition of 5 g/liter glycerol both improved production. The final levels of conversion achieved were >70% at a concentration of 40 g/liter and >50% at a concentration of 100 g/liter. The best conditions determined were then scaled up to a 1-liter fermentation that resulted in 55% conversion of 100 g/liter ribitol in 72 h, for a volumetric productivity of 17.4 g $liter^{-1}$ day^{-1}. This system represents a significantly improved method for the large-scale production of L-ribose.

Optically pure carbohydrates are important intermediates for the preparation of pharmaceutical, food, and agrochemical products (2, 4, 15, 22). In particular, these carbohydrates are increasingly important in biochemical research and in development of new pharmaceutical therapies since carbohydrates are involved in cellular recognition, signaling, extra- and intracellular targeting, and even the development of disease states (1, 2, 7, 22, 27). Access to consistent, optically pure, and inexpensive carbohydrate starting materials is critical to the continuation of this research.

The unique NAD-dependent mannitol-1-dehydrogenase (MDH) from *Apium graveolens* (33–38, 44) acts on the 1 position of D-mannitol, producing D-mannose (Fig. 1), in contrast to the more common 2-mannitol dehydrogenase, which interconverts D-mannitol and D-fructose (37). This novel regioselectivity combined with stringent stereoselectivity at the 2 position allows the MDH enzyme from *A. graveolens* to catalyze several interesting conversions, including the conversion of ribitol to L-ribose (Fig. 1), the conversion of D-sorbitol to L-gulose, and the conversion of galactitol to L-galactose (33). Sugars with the L configuration are often available only in limited amounts or at a high cost. To address these availability and economic concerns, utilization of MDH from *A. graveolens* is proposed.

For this study, L-ribose was chosen as a model target since it is the potential starting material for many L-nucleoside-based pharmaceutical compounds, including Clevudine, Tyzeka, Valtorcitabine, Elvucitabine, and Epivir (12, 14, 40). The interest in L-nucleosides has increased, as noted in Table 1, which shows several L-nucleoside-based pharmaceutical compounds recently approved or presently in clinical trials, creating a demand for L-ribose. Although several methods for the production of L-ribose have been described (19, 21, 31, 39), no method has provided an efficient and inexpensive source of L-ribose, as apparent from the increase in the bulk price (estimated at $1,000/kg, a price too high for intermediate-stage development) (29). With L-ribose selected as the model target for this platform technology, we created a novel recombinant *Escherichia coli* strain using a gene encoding the *A. graveolens* MDH. The recombinant MDH was characterized, and a process for whole-cell conversion was developed and improved, followed by liter scale production and isolation of L-ribose.

MATERIALS AND METHODS

Materials. Ribitol and L-ribose were purchased from CMS Chemicals Ltd. (Oxfordshire, United Kingdom), while oligonucleotide primers were obtained from Integrated DNA Technologies (Coralville, IA). Kanamycin, ampicillin, NAD, isopropyl-β-D-thiogalactopyranoside (IPTG), and lysozyme were obtained from Sigma-Aldrich (St. Louis, MO); other cell culture components were obtained from Difco (Sparks, MD). *E. coli* BL21(DE3), Rossetta(DE3), and Oragami (DE3) and the vectors pET26b and pET28a were purchased from Novagen (Madison, WI). *E. coli* W3110, DH5α, and BW25141 were obtained from CGSC (New Haven, CT), and *E. coli* EC100 was obtained from Epicentre (Madison, WI). An Aminex HPX 87P column (300 by 7.8 mm), a deashing cartridge (30 by 4.6 mm), and a Carbo-P microguard cartridge (30 by 4.6 mm) were purchased from Bio-Rad Laboratories, Inc. (Hercules, CA). Restriction enzymes EcoRI, HindIII, NdeI, and BamHI and T4 DNA ligase, as well as plasmid pMAL-C2X, were purchased from New England Biolabs (Ipswich, MA).

Cloning MDH. The MDH gene from *A. graveolens* was codon optimized and synthetically constructed by GeneArt (Toronto, Ontario, Canada) with flanking NdeI and HindIII restriction sites. The synthesized gene was digested with NdeI and HindIII and ligated into similarly prepared pMAL-C2x, pET26, pET28, and pTTQ18 using T4 DNA ligase at 16°C overnight. The ligation mixture was subsequently used to transform *E. coli* BL21(DE3). The MDH gene was then

* Corresponding author. Mailing address: zuChem, Rm. B107, 801 W. Main St., Peoria, IL 61606. Phone: (309) 495-7318. Fax: (309) 495-7319. E-mail: rwoodyer@zuchem.com.
† Present address: Pfizer, Inc., Groton, CT.
▽ Published ahead of print on 14 March 2008.

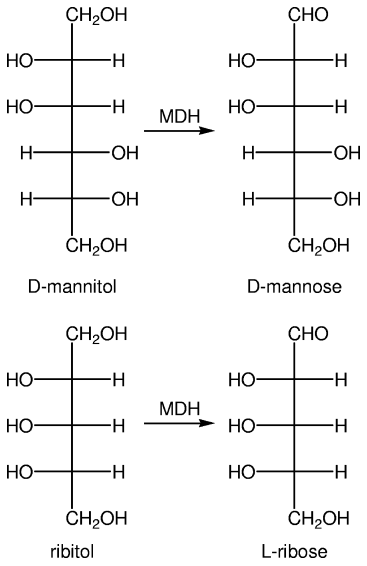

FIG. 1. MDH-catalyzed reactions. The MDH from *A. graveolens* catalyzes the unique conversion of D-mannitol to D-mannose and, similarly, the conversion of ribitol to L-ribose. The 2*R* stereochemistry is conserved for all of the MDH-catalyzed conversions.

amplified by PCR using forward primer 5′-AGA GGA ATT CGA ATG GCG AAA AGC AGC GAA AT-3′ (the underlined bases are an EcoRI restriction site) and reverse primer 5′-AGA GGG ATC CTT AAC GCG CCC AGG CTT TCT-3′ (the underlined bases are a BamHI restriction site). The resulting PCR product was digested with EcoRI and BamHI, ligated into pTRP338, and utilized to transform BL21(DE3). For construction of pMAL-MBP-MDH, the MDH gene was amplified by PCR using forward primer 5′-AGA GGG ATC CGA ATG GCG AAA AGC AGC GAA AT-3′ (the underlined bases are a BamHI restriction site) and reverse primer 5′-AGA GAA GCT TTT AAC GCG CCC AGG CTT TCT-3′ (the underlined bases are a HindIII restriction site). The resulting PCR product was digested with HindIII and BamHI, ligated into similarly prepared pMAL-C2X, and utilized to transform BL21(DE3). The NdeI-HindIII fragment of pMAL-MBP-MDH containing the maltose binding protein (MBP)-MDH fusion sequence was gel purified and ligated into similarly digested pET26 to obtain pET26-MBP-MDH. After BL21(DE3) clones for all of the desired constructs were obtained, correct clones were determined by restriction digestion analysis of purified plasmid and then sequenced at the University of Illinois-Urbana-Champaign Biotechnology Center. Clones with the correct sequence and restriction pattern were saved as frozen stocks at −80°C in LB containing 20% glycerol.

MDH expression. Overnight cultures in LB containing 100 μg/ml ampicillin (for pMAL-MBP-MDH, pMAL-MBP, and pTTQ18) or 50 μg/ml kanamycin (for pET26-MDH, pET26-MBP-MDH, pET28-H_6-MDH, pET28 negative control, and pTRP338) were incubated at 37°C with shaking. Fresh medium (5 ml) was inoculated with 200 μl of an overnight culture and grown for 1.5 h at 37°C. The temperature was then reduced to 25°C, and 0.5 mM IPTG was added. Shaking was continued for 4 h, and then cells were pelleted by centrifugation and resuspended in 1 ml 100 mM Tris buffer (pH 8.0) containing 1 mg/ml lysozyme and 0.2% Tween 80. The resuspended cells were frozen overnight at −20°C and thawed at room temperature. The cell lysate was clarified by centrifugation at 11,000 × *g* for 10 min at 4°C. The protein concentration of the clarified cell lysates was determined by the method of Bradford (11) using bovine serum albumin as a standard. Protein expression was visualized by sodium dodecyl sulfate-polyacrylamide gel electrophoresis (SDS-PAGE) by using the method of Laemmli (23) with lysate samples normalized to 10 μg of protein and Coomassie blue staining.

Purification of MBP-MDH. An overnight culture of BL21(DE3)/pMAL-MBP-MDH (5 ml) was used to inoculate 1.5 liters Terrific broth containing 20 mM glucose and 100 μg/ml ampicillin. After 3 h of incubation at 37°C, the temperature was reduced to 25°C and 0.5 mM IPTG was added. Cells (30 g) were harvested 5 h postinduction by centrifugation and resuspended in 90 ml of 50 mM HEPES (pH 7.2), 300 mM NaCl, 1 mg/ml lysozyme, and 10% glycerol and stored at −20°C. Dithiothreitol (DTT) was added to thawed cells (20 g) to a final concentration of 1 mM and sonicated for 5 min on ice (500 W, 50% amplitude, and 30% duty cycle). Cell debris was pelleted at 30,000 × *g* for 20 min, and the clarified lysate was loaded onto a 10-ml column of amylose resin equilibrated in 50 mM HEPES (pH 7.2), 300 mM NaCl, and 10% glycerol. The column was washed with 300 ml of equilibration buffer, and MBP-MDH was eluted in the same buffer containing 10 mM maltose. Pooled active fractions were desalted and concentrated using a Millipore Amicon 8400 stirred ultrafiltration cell with a YM10 membrane at 4°C with 20 mM Tris (pH 7.3), 50 mM NaCl, and 1 mM DTT. The enzyme concentration was determined by the method of Bradford (11) and by using UV (280 nm) with an estimated extinction coefficient (ε) of 93.7 mM^{-1} cm^{-1}. The preparation was stored in 10% glycerol at −80°C.

Characterization of MDH. The initial rates of reaction were determined by monitoring the increase in absorbance of NADH (ε = 6.22 mM^{-1} cm^{-1}) at 340 nm for 1 min at 25°C using a Beckman DU-62 spectrophotometer. Reactions were initiated by addition of ~25 μg of purified MBP-MDH or ~50 μg of partially purified lysate to 600 μl of 100 mM Tris buffer (pH 8.5) containing 500 mM D-mannitol and 2 mM NAD. To determine the effect of Zn^{2+}, 1, 10, 100, and 1,000 μM $ZnCl_2$ were added to the substrates. The effect of DTT was examined by adding 1 mM DTT to the substrate mixture. Substrate specificity was determined by adding partially purified lysate to 4 mM NAD and 150 mM D-mannitol, D-arabitol, erythritol, ribitol, D-sorbitol, xylitol, and galactitol in 100 mM bis-Tris buffer (pH 9.5). One unit of activity was defined as the production of 1 μmol NADH/min, and specific activity was defined as 1 U/mg of total protein added. All assays were performed in triplicate, and the means are reported below along with the associated standard deviations.

Flask conversion experiments. Whole-cell conversion experiments were carried out in 250-ml baffled flasks containing 100 ml LB with the appropriate antibiotic. Glycerol, ribitol, and $ZnCl_2$ were added from filter-sterilized stock solutions. The flasks were inoculated with 3 ml of an overnight culture and incubated at 37°C for 3 h; the temperature was then reduced to 25°C, and 0.5 mM IPTG was added. The pH was maintained above 6.0 using 50% NH_4OH. Samples were taken at regular intervals after inoculation and analyzed by high-performance liquid chromatography (HPLC). Experiments were performed in triplicate, and the means are reported below along with the associated standard deviations.

Fermentor conversion experiments. Fermentors with a 2-liter capacity (Biostat B; B. Braun Biotech International, Allentown, PA) were used with 1 liter of LB containing 100 mg ampicillin. Ribitol was sterilized separately from the medium and pumped into the fermentor along with 20 g of glycerol and 4 drops of antifoaming agent. A 50-ml inoculum from an overnight *E. coli*/pMAL-MBP-MDH culture was used to start the conversion. The fermentation preparations were mixed at 1,000 rpm, the aeration rate was 1 liter/min, the temperature was controlled at 37°C, and the pH was maintained above 6.0 with 50% NH_4OH.

TABLE 1. Examples of L-nucleoside-based pharmaceuticals

Trade name	Company	Conditions[a]	Starting materials	Status
Tyzeka	Idenix Pharmaceuticals	HBV	L-Ribose, L-arabinose	Approved
Valtorcitabine	Idenix Pharmaceuticals	HBV	L-Ribose, L-arabinose	Phase II
Clevudine	Pharmasset	HBV	L-Ribose, L-arabinose, L-xylose	Phase III
Epivir	GSK	HIV	L-Gulose, L-mannose, L-galactose	Approved
Elvucitabine	Achillion	HIV, HBV	L-Xylose, D-glutamate	Phase II
Emtriva	Gilead	HIV, HBV	L-Gulose, L-mannose, L-galactose	Approved
Pentacept	Pharmasset	HBV	L-Gulose, L-mannose, L-galactose	Preclinical

[a] HBV, hepatitis B virus; HIV, human immunodeficiency virus.

```
      M  A  K  S  S  E  I  E  H  P  V  K  A  F  G  W  A  A  R  D
1     atggcgaaaagcagcgaaatcgaacacccggtgaaagcgtttggttgggcggcacgtgat  60
      T  T  G  L  L  S  P  F  K  F  S  R  R  A  T  G  E  K  D  V
61    accaccggtctgctgagcccgttcaaatttagccgtcgcgcgaccggcgaaaaagatgtg  120
      R  L  K  V  L  F  S  G  V  C  H  S  D  H  H  M  I  H  N  N
121   cgcctgaaagtgctgtttagcggcgtgtgccacagcgatcaccacatgatccacaacaac  180
      W  G  F  T  T  Y  P  I  V  P  G  H  E  I  V  G  V  V  T  E
181   tggggcttcaccacctatccgatcgtgccgggccatgaaattgtgggcgtggtgaccgaa  240
      V  G  S  K  V  E  K  V  K  V  G  D  N  V  G  I  G  C  L  V
241   gtgggcagcaaagtggaaaaagtgaaagtgggcgataacgtgggcattggctgcctggtt  300
      G  S  C  R  S  C  E  S  C  C  D  N  R  E  S  H  C  E  N  I
301   ggtagctgccgtagctgcgaaagctgctgcgataaccgcgaaagccactgcgaaaacatc  360
      I  D  T  Y  G  S  I  Y  F  D  G  T  M  T  H  G  G  Y  S  D
361   atcgatacctacggcagcatctacttcgatggcaccatgacccatggcggctacagcgat  420
      T  M  V  A  D  E  H  F  I  L  R  W  P  K  N  L  P  L  D  S
421   accatggtggcggatgaacacttcattctgcgctggccgaaaaacctgccgctggattct  480
      G  A  P  L  L  C  A  G  I  T  T  Y  S  P  L  K  Y  Y  G  L
481   ggtgcaccgctgctgtgtgcgggcattaccacctacagcccgctgaaatactacggcctg  540
      D  K  P  G  T  K  I  G  V  V  G  L  G  G  L  G  H  V  A  V
541   gataaaccgggcaccaaaatcggtgtggtgggcctgggtggtctgggtcatgtggcggtg  600
      K  M  A  K  A  F  G  A  Q  V  T  V  I  D  I  S  E  S  K  R
601   aaaatggcgaaagcgttcggtgcgcaggtgaccgtgatcgatatcagcgaaagcaaacgc  660
      K  E  A  L  E  K  L  G  A  D  S  F  L  L  N  S  D  Q  E  Q
661   aaagaagcgctggaaaaactgggcgcggatagcttcctgctgaacagcgatcaagaacag  720
      M  K  G  A  R  S  S  L  D  G  I  I  D  T  V  P  V  N  H  P
721   atgaaaggcgcgcgtagcagcctggatggcattatcgataccgtgccggtgaatcatccg  780
      L  A  P  L  F  D  L  L  K  P  N  G  K  L  V  M  V  G  A  P
781   ctggcgccgctgttcgatctgctgaaaccgaacggcaaactggtgatggttggtgcgccg  840
      E  K  P  F  E  L  P  V  F  S  L  L  K  G  R  K  L  L  G  G
841   gaaaaaccgttcgaactgccggtgttcagcctgctgaaaggccgtaaactgctgggcggc  900
      T  I  N  G  G  I  K  E  T  Q  E  M  L  D  F  A  A  K  H  N
901   accattaacggcggcatcaaagaaacccaggaaatgctggatttcgcggcgaaacacaac  960
      I  T  A  D  V  E  V  I  P  M  D  Y  V  N  T  A  M  E  R  L
961   atcaccgcggatgtggaagtgatcccgatggattacgtgaacaccgcgatggaacgcctg 1020
      V  K  S  D  V  R  Y  R  F  V  I  D  I  A  N  T  M  R  T  E
1021  gtgaaaagcgatgtgcgctaccgcttcgtgattgatatcgcgaatacgatgcgtaccgaa 1080
      E  S  L  G  A  *
1081  gaaagcctgggcgcgtaa  1098
```

FIG. 2. Optimized coding sequence for MDH expression in *E. coli*. Approximately 26% of the coding nucleotides were changed without modification of the encoded protein sequence.

$ZnCl_2$ was added to a final concentration of 0.5 or 0.05 mM from a sterilized stock solution. After 3 h or when a cell dry weight (CDW) of approximately 1.2 g/liter was reached, the temperature was reduced to 25 or 27.5°C, and IPTG was added to a final concentration of 0.5 mM. During the run the dissolved oxygen concentration, pH, and temperature were continuously monitored. Samples were taken at regular time intervals and analyzed by HPLC.

Analysis. The HPLC separation system consisted of a solvent delivery system (P2000 pump; Spectra-Physics, San Jose, CA) equipped with an autosampler (717; Waters Chromatography Division, Millipore Corp., Milford, MA), a refractive index detector (410 differential refractometer; Waters), and a computer software-based integration system (Chromquest 4.0; Spectra-Physics). An ion-moderated partition chromatography column (Aminex HPX-87P with deashing and Carbo-P microguard cartridges) was utilized at 85°C with a mobile phase of Milli-Q-filtered water at a flow rate of 0.6 ml/min. Peaks were detected by using the refractive index and were identified and quantified by comparison of the retention times to the retention times of authentic standards (ribose and ribitol). Optical density measurements were taken using a Beckman DU-62 spectrophotometer and were converted into CDW as previously described (25).

Purification of L-ribose. The L-ribose produced was purified. Cells were removed from the culture by centrifugation, and the medium was treated with 2% (wt/vol) activated carbon at 60°C for 1 h. The mixture was filtered to remove the carbon and evaporated to obtain 30 to 50% solids under a vacuum. The mixture was then separated using Dowex 50x-400 cation-exchange resin in the calcium form with water as the mobile phase. Ribose (D/L) was eluted last, and fractions containing pure ribose were identified by HPLC and combined. The pooled fractions were evaporated to obtain approximately 80% solids, seeded with L-ribose crystals, and allowed to crystallize for several days at 4°C. The crystalline product was washed with ice-cold ethanol and dried. Polarimetry was carried out with a 10% solution of recovered ribose crystals or L-ribose standard in water using a Perkin-Elmer 241 polarimeter at 25°C with a 1-dm quartz cell and a deuterium lamp with emission at 589 nm.

RESULTS AND DISCUSSION

Expression and activity of recombinant MDH. Our novel platform for the production of L-sugars takes advantage of the unique NAD-dependent MDH from *A. graveolens* (33, 36–38), which has a preference for the 2*R* configuration of the resulting aldose (33). To create an *E. coli* strain for the direct conversion of ribitol into L-ribose, the *A. graveolens* MDH gene was codon optimized for expression in *E. coli* and synthetically constructed (GeneArt, Toronto, Ontario, Canada). The optimized MDH gene (Fig. 2) was subcloned into several *E. coli* expression vectors, including three IPTG-inducible T7 promoter vectors (pET28 constructed as an N-terminal His-tagged fusion and pET26 constructed both with and without an N-terminal MBP fusion), three IPTG-inducible Tac promoter vectors (pMAL constructed with and without an N-terminal MBP fusion and pTTQ18 constructed with no fusion), and one constitutive expression Trp promoter vector (pTRP).

MDH expression was checked by SDS-PAGE for *E. coli* BL21(DE3) transformed with each of these vectors (Fig. 3A). The optimized MDH gene was expressed well, with a clear

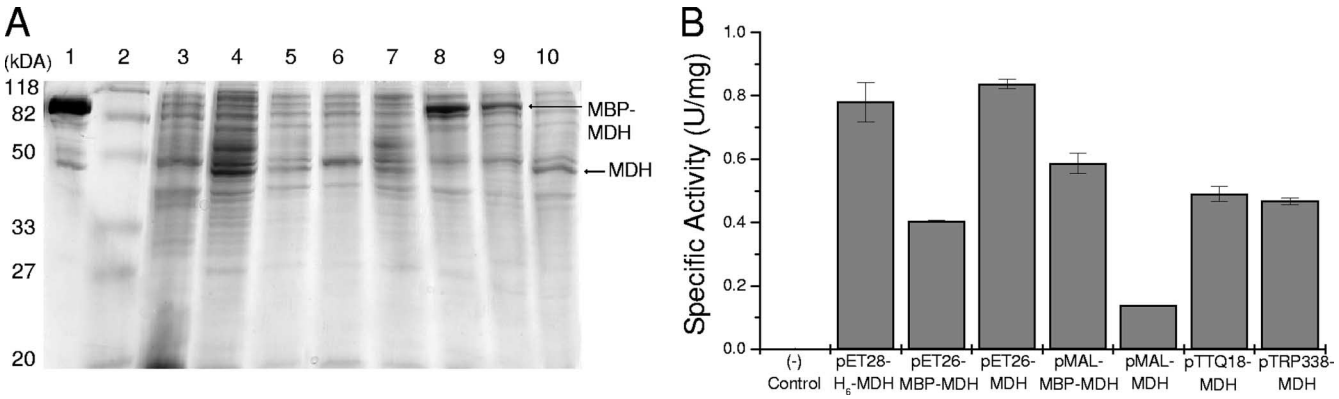

FIG. 3. Expression and activity of MDH. (A) Expression of MDH in several expression vectors and purity of MBP-MDH as analyzed by SDS-PAGE. Lane 1, purified MBP-MDH; lane 2, size marker; lane 3, pET28 negative control; lane 4, pTRP-MDH; lane 5, pTTQ18-MDH; lane 6, pET28-H_6-MDH; lane 7, pMAL-MDH; lane 8, pMAL-MBP-MDH; lane 9, pET26-MBP-MDH; lane 10, pET26-MDH. (B) Specific activity of MDH from partially purified lysates measured with ribitol as the substrate. The expression of pMAL-MBP-MDH appeared to be the highest, while the pET system vectors provided slightly higher activity.

band visible by SDS-PAGE corresponding to an expected monomer size of 39.7 kDa for pTRP-MDH, pTTQ18-MDH, pMAL-MDH, and pET26-MDH (Fig. 3A, lanes 4, 5, 7, and 10, respectively), 42.2 kDa for the His-tagged fusion expressed from pET28-H_6-MDH (Fig. 3A, lane 6), or 82.8 kDa for pET26-MBP-MDH and pMAL-MBP-MDH (Fig. 3A, lanes 8 and 9). The expression level of MDH in *E. coli* was variable depending on the expression vector used, with the highest expression accounting for approximately 50% of the total soluble protein for pMAL-MBP-MDH expression. Interestingly, the lowest expression level was that of pMAL-expressed native MDH, which accounted for less than 10% of the total soluble protein. This suggested that even though the gene sequence had been optimized for *E. coli*, the protein expression was still significantly improved by fusion to the highly soluble and expressed MBP. It was also found that, in addition to being readily expressed in *E. coli*, the MBP-MDH fusion could be readily purified in a single step as described in Materials and Methods. The resulting protein was >95% pure, and only minor impurities were found when SDS-PAGE samples were overloaded (Fig. 3A, lane 1). Approximately 15 mg of purified MBP-MDH protein could be obtained from 1 liter of expressed culture by this method.

Activity, substrate specificity, and small-molecule effects on recombinant MDH. The MDH gene was expressed in *E. coli*; however, many eukaryotic proteins are not actively expressed in bacterial systems, or the resulting protein is active but has modified properties due to different posttranslational modifications or cellular environments (3, 9, 17, 32). Furthermore, several of the constructs created result in fusion protein products, which could also alter the activity of the expressed MDH (5, 6). Therefore, enzyme activity was determined for each of the partially purified *E. coli* cell lysates and the purified MBP-MDH (Fig. 3B). Each of the expression strains did indeed express active MDH. The highest specific activity was achieved with the vectors pET26-MDH and pET28-H_6-MDH, and the N-terminal His tag had no significant effect. The activity of pMAL-MBP-MDH-expressed protein was a close third. To determine the effect of temperature on active expression, cell lysate was prepared from cells containing pTRP-MDH expressed at 16, 25, 30, and 37°C; the best activity resulted from expression at 25°C, while at 37°C the activity was approximately threefold lower and at 16°C the activity was fivefold lower. The activity results plainly demonstrated that the recombinant MDH could be actively expressed in *E. coli* from a variety of different expression systems, and the high activities observed with cell lysates were promising for the intended whole-cell conversions. The results for the temperature of induction suggest that the MDH protein folding may limit activity, since the folding of proteins that tend to misfold or form inclusion bodies is typically enhanced in *E. coli* when the proteins are expressed at a lower temperature (5, 6). This suggestion is also supported by the large difference in active expression of pMAL-MBP-MDH and pMAL-MDH, since fusion of MBP is well known to improve folding and soluble expression (6, 20).

The specific activity of the purified MBP-MDH was 3.24 ± 0.03 U/mg, and when the protein mass was corrected for the MBP fusion, the specific activity was 6.36 ± 0.06 U/mg of MDH subunit. The corrected specific activity compares favorably with that of the multistep-purified preparation from celery suspension cultures, 6.1 U/mg (38). Thus, the recombinant MDH protein maintains a similar level of activity, while the ease and speed of *E. coli* culture, simple expression, and one-step purification make access to this enzyme much easier for in vitro enzymatic bioconversion studies. However, the purified recombinant MDH is a rather large MBP fusion protein and is expressed in a very different cellular environment, and it may have different characteristics than the native nonfusion MDH protein previously described (33–38). Therefore, the recombinant enzyme was tested with several substrates, as shown in Table 2. The recombinant MDH enzyme from *E. coli* had substrate specificity very similar to that of the native enzyme (33). The most notable differences are that the recombinant MDH had 10% higher relative activity with ribitol and 13% lower relative activity with D-sorbitol than the native enzyme. It is unclear whether these differences are statistically significant as associated errors were not provided in the previous study (33); however, the higher relative activity with ribitol is beneficial for production of L-ribose, while the broad substrate

TABLE 2. Substrate specificity of recombinant and native MDH

Substrate	Product	Recombinant MDH activity (%)[a]	Native MDH activity (%)[b]
D-Mannitol	D-Mannose	100	100
D-Arabitol	D-Lyxose	38	37
Erythritol	L-Erythrose	9	16
Ribitol	L-Ribose	47	36
D-Sorbitol	L-Gulose	9	22
Xylitol	L-Xylose	3	0
Galactitol	L-Galactose	23	26

[a] Standard deviations, ≤2%.
[b] Previously determined (33).

specificity should allow this system to be utilized for the synthesis of many L-sugars.

The effects of DTT and Zn^{2+} on the activity of recombinant MDH were also investigated, since previously the native enzyme was shown to be inhibited by the reducing reagent DTT, with 50% inactivation at a concentration of 0.6 mM, and almost completely inactivated by addition of 1 mM Zn^{2+} (36). Somewhat different results were obtained with the recombinant MDH preparation. The enzyme as we purified it was not inactivated by DTT; rather, a slight increase in activity (25% ± 2%) was observed in the presence of 1 mM DTT. Perhaps this was due to variation in folding or posttranslational modification, or perhaps the affected residues of the native enzyme could be partially protected by the large MBP fusion of the recombinant enzyme. Addition of 1 mM Zn^{2+} to the recombinantly produced enzyme resulted in a nearly complete loss of activity, corroborating the previous results (36); however, in the presence of 1 μM Zn^{2+} there was a twofold increase in specific activity, and in the presence of 10 μM Zn^{2+} there was a twofold decrease in activity. These results suggest that MDH has tightly bound Zn^{2+}, as the unusual activity profile with increasing concentrations is typical of Zn^{2+}-dependent alcohol dehydrogenases and other proteins containing tightly bound zinc (41). At low concentrations the zinc ion activates the enzyme, but at higher concentrations loss of activity is due to random coordination with histidine and cysteine residues. This conclusion is further supported by the presence of a conserved Zn^{2+} binding domain in MDH (36).

Flask production of L-ribose. We next studied the optimized MDH system in *E. coli* BL21 using pMAL-MBP-MDH for whole-cell L-ribose production. Transport was not expected to be an issue as ribitol has been shown to be passively transported by the glycerol facilitator of *E. coli* (16) and neither B nor K-12 stains metabolize ribitol (28). Indeed, the results were very promising; at an initial ribitol concentration of 40 g/liter L-ribose accumulated in the medium for the first 72 h, and then the amount leveled off to a final conversion of 41% ± 2% at 144 h, for a volumetric productivity of 2.8 ± 0.1 g liter^{-1} day^{-1}. The CDW reached 2.8 g/liter at 24 h and remained at that level ±5% for the remainder of the experiment. No significant consumption of either L-ribose or ribitol occurred. Furthermore, the ribose produced was isolated and analyzed by polarimetry, which verified that it was indeed L-ribose with an optical rotation ($[\alpha]^D$) of −19.5, matching that of an L-ribose standard.

Several steps were subsequently taken to improve the L-ribose production in shaken flasks. Addition of a carbon source, such as glucose or glycerol, was hypothesized to improve conversion due to higher cell densities. Therefore, the whole-cell conversion experiment was repeated with addition of 5 g/liter glycerol or 5 g/liter glucose. The cell mass obtained proved to be significantly higher for both the glycerol- and glucose-containing flasks, and the CDW at 24 h were 4.5 and 4.8 g/liter, respectively; however, only in the flask containing glycerol was there statistically higher conversion (51% ± 3%) or volumetric productivity (3.4 ± 0.2 g liter^{-1} day^{-1}). To further highlight the difference, the specific conversion rates were calculated for the period of fastest conversion (24 to 48 h) for LB (1.6 ± 0.1 g L-ribose g cells^{-1} day^{-1}), LB containing glycerol (1.7 ± 0.1 g L-ribose g cells^{-1} day^{-1}), and LB containing glucose (1.1 ± 0.1 g L-ribose g cells^{-1} day^{-1}). Based on similar specific conversion, increased cell density alone was a satisfactory explanation for the improved conversion and productivity with glycerol, but it did not explain the reduction in specific conversion with glucose. *E. coli* growth on glycerol is known to result in an increased level of a glycerol facilitator, which can transport ribitol (16); however, many other carbon sources, including glucose, decrease the level of this channel (30, 43). Thus, the best explanation is that glycerol has the effect of increasing cell density while maintaining levels of the glycerol facilitator to aid ribitol transport. An additional effect was identified as flasks containing an added carbon source converted ribitol more slowly for the first 24 h, corresponding to the consumption of the added carbon source, which was followed by a more rapid stage (Fig. 4A). This can be explained by the fact the addition of a carbon source to complex media is known to significantly raise the NADH/NAD ratio (10) during consumption, which would inhibit the NAD-dependent MDH conversion.

We determined that MDH activity in vitro is positively influenced by addition of 1 μM Zn^{2+} but negatively influenced by higher Zn^{2+} concentrations, suggesting that the enzyme as purified is not completely occupied by Zn^{2+}. The intracellular zinc concentration is tightly controlled in the femtomolar range, meaning that free Zn^{2+} is essentially not available, although the total zinc quota (bound) is around 200 μM for *E. coli* (26). The recombinant MBP-MDH fusion protein reaches intracellular concentrations greater than 13 μM based on the amount of recovered protein and an assumed aqueous cell volume of 7×10^{-16} liter. Thus, it was hypothesized that Zn^{2+} limitation might affect the production strain and that addition of Zn^{2+} to LB, which contains only ~10 μM zinc (24), might result in better conversion. To test this hypothesis, a range of Zn^{2+} concentrations were added to LB and tested using a more challenging bioconversion of 100 g/liter of ribitol with inclusion of 5 g/liter glycerol (Fig. 4B). Without any additional Zn^{2+} the level of conversion reached 46% ± 2% in 240 h, for a volumetric productivity of 4.6 ± 0.2 g liter^{-1} day^{-1}. Intriguingly, addition of 50 μM Zn^{2+} improved the level of conversion to 50% ± 3%, while addition of 150 μM further improved the level of conversion to 52% ± 3% and addition of 500 μM Zn^{2+} resulted in 54% ± 3% conversion and the best volumetric productivity, 5.4 ± 0.3 g liter^{-1} day^{-1}. At Zn^{2+} concentrations as high as 0.5 mM cell growth was not significantly affected, correlating well to previous research on the Zn^{2+} dependence of *E. coli* growth in LB (8). However, at 1.5 mM

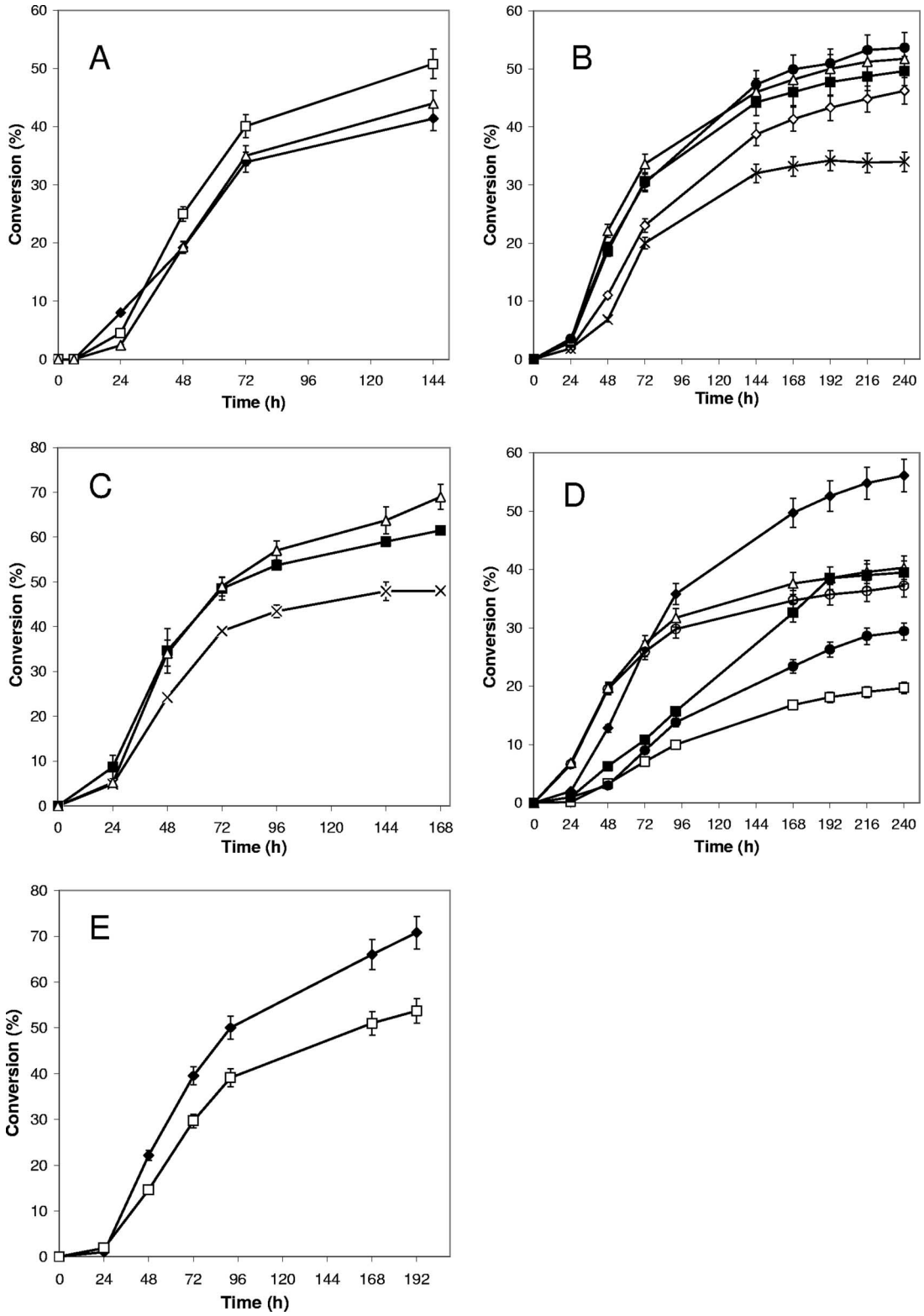

FIG. 4. L-Ribose shaken flask bioconversions using *E. coli*. (A) Conversion of 40 g/liter ribitol using *E. coli* pMAL-MBP-MDH in LB without an added carbon source (◆), with 5 g/liter glycerol (□), and with 5 g/liter glucose (△). (B) Effect of the following Zn^{2+} concentrations on conversion of 100 g/liter ribitol by *E. coli* pMAL-MBP-MDH with 5 g/liter glycerol: 0 mM (◇), 0.05 mM (■), 0.15 mM (△), 0.5 mM (●), and 1.5 mM (×). (C) Effect of the following Zn^{2+} concentrations on conversion of 40 g/liter ribitol by *E. coli* pMAL-MBP-MDH with 5 g/liter glycerol: 0 mM (×), 0.05 mM (■), and 0.20 mM (△). (D) Conversion of 100 g/liter ribitol with 0.5 mM Zn^{2+} and 5 g/liter glycerol with different *E. coli* expression vector systems, including pMAL-MDH (□), pTRP338-MDH (●), pTTQ18-MDH (■), pET26-MBP-MDH (○), pET26-MDH (△), and pMAL-MBP-MDH (◆). (E) Conversion of 100 g/liter ribitol (□) or 40 g/liter ribitol (◆) by *E. coli* pMAL-MBP-MDH in the presence of 0.5 mM Zn^{2+} and 5 g/liter glycerol.

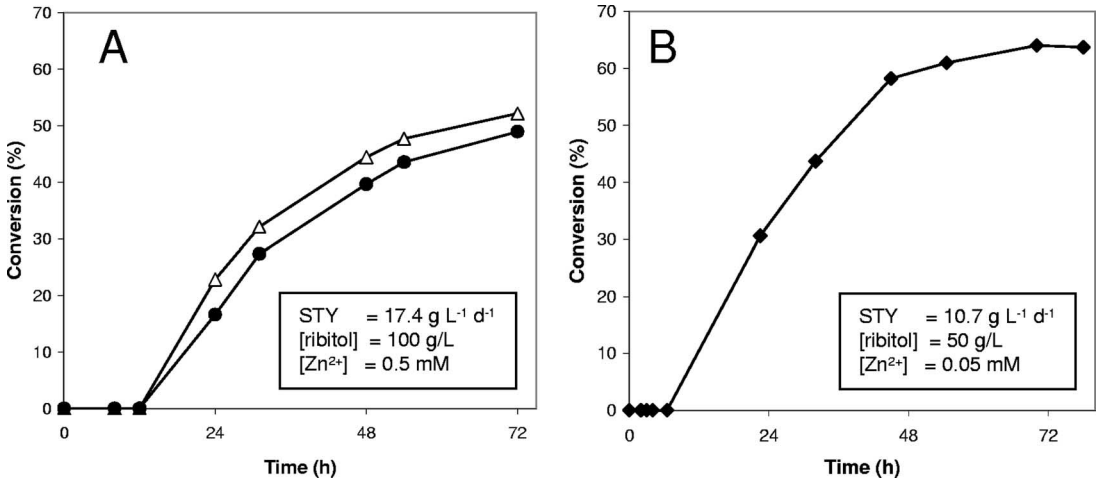

FIG. 5. L-Ribose production in 1-liter fermentations. (A) Two fermentations were carried out with 0.5 mM Zn^{2+}, 100 g/liter ribitol, and 20 g/liter glycerol. One fermentation was carried out at 25°C (●), and the other was carried out at 27.5°C (△). The higher temperature resulted in slightly greater productivity. The levels of conversion were 49 g/liter at 25°C and 52 g/liter at 27.5°C, resulting in space time yields (STY) of 16.3 g $liter^{-1}$ day^{-1} and 17.4 g $liter^{-1}$ day^{-1}. (B) A third fermentation (◆) was carried out at 25°C with lower concentrations of starting material (50 g/liter ribitol) and Zn^{2+} (0.05 mM). The result was a higher level of conversion (64%) but a lower space time yield (10.7 g $liter^{-1}$ day^{-1}). All three fermentations had an initial phase with slower conversion corresponding to glycerol consumption.

Zn^{2+} the cell doubling time was significantly higher, as also previously described (8), and the level of conversion was lower, 34%. Addition of 5 mM Zn^{2+} inhibited cell growth altogether, with no discernible conversion. Addition of Zn^{2+} to LB had a more significant impact at a ribitol concentration of 40 g/liter, as shown in Fig. 4C. In this experiment, addition of 0, 50, and 200 μM Zn^{2+} resulted in levels of conversion of 48% ± 2%, 59% ± 1%, and 64% ± 3%, respectively, while no effect on growth or the final CDW was discernible. Although it cannot be directly concluded from these data that the observed improvements were due to higher zinc content of MDH, addition of Zn^{2+} to the media at micromolar concentrations had a significant positive effect on the production of L-ribose, and Zn^{2+} supplementation was used throughout the remaining experiments.

Whole-cell bioconversions were carried out under the best conditions identified (0.5 mM Zn^{2+}, 100 g/liter ribitol, and 5 g/liter glycerol) for six of the created expression strains harboring pMAL-MDH, pTRP338-MDH, pTTQ18-MDH, pET26-MBP-MDH, pET26-MDH, or pMAL-MBP-MDH, as shown in Fig. 4D. Although the specific activity of the crude extract was highest with pET26-MDH, surprisingly, these conditions did not result in the best conversion, which stopped at a level of 40% ± 2%. Similar results were observed for pET26-MBP-MDH. The high initial activity followed by a steep drop-off was likely a function of the T7 expression system, which is very rapid and efficient but typically not stable after induction. The vector originally chosen for the best protein expression (pMAL-MBP-MDH) resulted in the highest level of conversion, 55% ± 3%, and the vector with the lowest protein expression (pMAL-MDH) had the lowest level of conversion, 20% ± 1%. From these results, one could conclude that steady high-level expression is important for conversion and that the conversion is likely limited by MDH activity, since the differences are readily correlated to expression and activity levels. To ascertain if there are strain-related limitations, *E. coli* BL21 was compared to several other *E. coli* strains, including BW25141, W3110, Oragami, Rosetta, DH5α, and EC100 with pMAL-MBP-MDH, under the best conditions for bioconversion. However, the results were similar to (BW25141 and W3110) or worse than (Oragami, Rosetta, DH5α, and EC100) the results obtained with BL21 and were not investigated further (data not shown).

Figure 4E shows the bioconversion progress for 40 and 100 g/liter ribitol using the best conditions (5 g/liter glycerol and 0.5 mM Zn^{2+}). At 40 g/liter a very high level of conversion, 71% ± 4%, was achieved at 192 h, for a volumetric productivity of 3.6 ± 0.2 g $liter^{-1}$ day^{-1}. Thus, a very robust whole-cell L-ribose production system had been created and optimized to levels of conversion of 71% ± 4% at 40 g/liter ribitol and 55% ± 3% at 100 g/liter ribitol.

Bioreactor Production of L-ribose. L-Ribose production on a small scale exceeded expectations and proved to be very tunable. To determine if the system was scalable and if the productivity could be improved further, aerobic fermentation was attempted. Two fermentations were carried out with 0.5 mM Zn^{2+}, 100 g/liter ribitol, and 20 g/liter glycerol; one fermentation was carried out at 25°C, and the other was carried out at 27.5°C (Fig. 5A). The slow phase of the conversion was much more pronounced in these fermentations due to the use of 20 g/liter glycerol and thus a longer consumption time; however, after the glycerol was consumed, the conversion rate was significantly higher until conversion ceased around 72 h. The higher temperature resulted in slightly higher levels of conversion and productivity (52% and 17.4 g $liter^{-1}$ day^{-1}, respectively). The lower-temperature fermentation reached completion at 49% conversion and a volumetric productivity of 16.3 g $liter^{-1}$ day^{-1}. A third fermentation was carried out with lower levels of starting material (50 g/liter ribitol) and Zn^{+2} (0.05 mM), which resulted in a higher level of conversion (64%) (Fig. 5B) but a lower volumetric productivity (10.7 g $liter^{-1}$ day^{-1}). All three fermentations had an initial slow phase cor-

responding to glycerol consumption, during which a small amount (~1 ml) of 50% NH_4OH was used to maintain the pH. Once the glycerol was consumed, the CDW reached approximately 12 g/liter, after which the cell growth stopped and conversion was rapid. L-Ribose was easily isolated from the fermentations by removing the cells and concentrating the supernatant, followed by cation-exchange chromatography, concentration, and crystallization. Greater than 75% of the final product was generally recovered, and this product had a melting point and optical rotation similar to the melting point and optical rotation of an authentic sample of L-ribose.

While several synthetic routes for producing L-ribose have been explored, each of these routes has fundamental flaws. There is a chemical process to convert D-mannono-1,4-lactone to L-ribose (39). However, this process requires eight synthetic steps and has an overall L-ribose yield of 51%. An improved process using the same starting material has been described, which requires six steps that result in an overall yield of 68% (31). Both processes are too costly for large-scale L-ribose production, especially considering the increasing cost of the D-mannose required to produce D-mannono-1,4-lactone (29). The conversion of L-arabinose to L-ribose can be carried out utilizing xylose isomerase (18) or molybdic acid (19). Using xylose isomerase, the conversion is slow and the volumetric productivity is 5.2 g liter^{-1} day^{-1} (18), and this method additionally requires the use of large amounts of cross-linked enzyme crystals. The molybdic acid route results in inefficient conversion to L-ribose (22.6%), but the volumetric productivity is higher, 480 g liter^{-1} day^{-1}. Unfortunately, L-arabinose at the bulk level is not inexpensive; the estimated price is $100/kg. This process requires extensive purification to remove remaining starting material, and additional environmental issues make this process unattractive. There is a separate process that produces L-ribose from the L-arabinose extracted from natural sources, such as biomass (42). However, this process requires extensive and expensive purification technologies (42). For comparison, the MDH-based system described here at the very beginning of process optimization allows simple isolation of L-ribose, has more than threefold-better productivity than the xylose isomerase process, and has a much better level of conversion than the molybdic acid process without similar environmental hazards. Additionally, our MDH-based conversion system uses ribitol as a starting material, which can be created cheaply by chemical or whole-cell reduction of D-ribose (~$20 to 30/kg) or by direct fermentation from glucose using a variety of osmophilic yeasts (1, 13, 21).

A fermentative route that uses a *Trichosporonoides* strain to produce ribitol from D-glucose, a *Gluconobacter* strain that oxidatively produces L-ribulose from ribitol, and a *Cellulomonas* strain to isomerize the L-ribulose to L-ribose has been described (21). While D-glucose is an inexpensive starting material, the cost of the three sequential and separate fermentations is prohibitive, and the final level of conversion to L-ribose is only 18%. Additionally, the *Trichosporonoides* fermentation is slow and difficult, having a total fermentation time of approximately 9 days and requiring many steps that result in a volumetric productivity of just 1.1 g liter^{-1} day^{-1}. It is difficult to dissect this process for a direct comparison starting at ribitol, since the same medium is used throughout the process. However, if the process was to start using ribitol as the process described in this paper does, the calculated productivity is 10.7 g liter^{-1} day^{-1} and the level of conversion is 49%. The *E. coli* fermentation described in this study represents a significant improvement in terms of the conversion, volumetric productivity, and simplicity of the process.

The value of the technology presented in this paper goes beyond L-ribose production. It is likely that the recombinant strains created here will serve as an enabling technology for the production of other L-sugars from inexpensive polyols, as shown in Table 2. All of these compounds are (Table 1) or could be used in biochemical or pharmaceutical applications (1, 29, 31), but many are simply not economically available in the quantities needed for studies. The number of L-nucleoside-based pharmaceuticals in clinical trials now (Table 1) clearly demonstrates the need for access to the rare sugars accessible with the MDH system. Additionally, advances in glycosylation technology have resulted in a multitude of drug discovery projects requiring L-sugar starting units.

To summarize, an enzyme with a novel MDH activity originating from garden celery was recombinantly expressed in *E. coli*. The recombinant enzyme was readily purified and had activity and substrate specificity similar to the activity and substrate specificity of the native enzyme. Whole-cell conversion of ribitol to L-ribose was demonstrated using the recombinant *E. coli* strains with volumetric productivities that were as high as 17.4 g liter^{-1} day^{-1} and levels of conversion as high as 71% ± 4%. This fermentation route to L-ribose would solve many of the problems associated with other methods by using a single-step synthesis, inexpensive starting material, and green bioconversion.

ACKNOWLEDGMENTS

We acknowledge Greg Kennedy and Melissa Tisoncik for their excellent technical assistance.

This work was supported by a small business innovative research grant from the National Institutes of Health.

Mention of trade names or commercial products is solely for the purpose of providing specific information and does not imply recommendation or endorsement by the U.S. Department of Agriculture.

REFERENCES

1. **Ahmed, Z.** 2001. Production of natural and rare pentoses using microorganisms and their enzymes. Electron. J. Biotechnol. **4:**103–110.
2. **Allen, J. R., C. R. Harris, and S. J. Danishefsky.** 2001. Pursuit of optimal carbohydrate-based anticancer vaccines: preparation of a multiantigenic unimolecular glycopeptide containing the Tn, MBr1, and Lewis(y) antigens. J. Am. Chem. Soc. **123:**1890–1897.
3. **Andersen, D., and L. Krummen.** 2002. Recombinant protein expression for therapeutic applications. Curr. Opin. Biotechnol. **13:**117–123.
4. **Ashurst, P. (ed.).** 2005. Chemistry and technology of soft drinks and fruit juices. Blackwell Publishing, Oxford, United Kingdom.
5. **Baneyx, F.** 1999. In vivo folding of recombinant proteins in *Escherichia coli*, p. 551–565. *In* A. L. Demain and J. Davies (ed.), Manual of industrial microbiology and biotechnology, 2nd ed. ASM Press, Washington, DC.
6. **Baneyx, F.** 1999. Recombinant protein expression in *Escherichia coli*. Curr. Opin. Biotechnol. **10:**411–421.
7. **Bartolozzi, A., and P. H. Seeberger.** 2001. New approaches to the chemical synthesis of bioactive oligosaccharides. Curr. Opin. Struct. Biol. **11:**587–592.
8. **Beard, S. J., R. Hashim, J. Membrillo-Hernandez, M. N. Hughes, and R. K. Poole.** 1997. Zinc(II) tolerance in *Escherichia coli* K-12: evidence that the zntA gene (o732) encodes a cation transport ATPase. Mol. Microbiol. **25:** 883–891.
9. **Bernhard Fischer, I. S., and P. Goodenough.** 1993. Isolation, renaturation, and formation of disulfide bonds of eukaryotic proteins expressed in *Escherichia coli* as inclusion bodies. Biotechnol. Bioeng. **41:**3–13.
10. **Berrios-Rivera, S. J., A. M. Sanchez, G. N. Bennett, and K. Y. San.** 2004. Effect of different levels of NADH availability on metabolite distribution in *Escherichia coli* fermentation in minimal and complex media. Appl. Microbiol. Biotechnol. **65:**426–432.

11. **Bradford, M. M.** 1976. A rapid and sensitive method for the quantitation of microgram quantities of protein utilizing the principle of protein-dye binding. Anal. Biochem. **72:**248–254.
12. **Casey, J., B. Korba, P. Cote, J. Gerin, B. Tennant, and C. Chu.** December 2003. Method of treating hepatitis delta virus infection. U.S. patent 6,670,342.
13. **Chida, S.** April 2001. Microorganism and a process for producing polyols by using the same. U.S. patent 6,214,605.
14. **Doong, S., C. Tsai, R. Schinazi, D. Liotta, and Y. Cheng.** 1991. Inhibition of the replication of hepatitis B virus in vitro by 2′,3′-dideoxy-3′-thiacytidine and related analogues. Proc. Natl. Acad. Sci. USA **88:**8495–8499.
15. **Griffith, B. R., J. M. Langenhan, and J. S. Thorson.** 2005. 'Sweetening' natural products via glycorandomization. Curr. Opin. Biotechnol. **16:**622–630.
16. **Heller, K. B., E. C. Lin, and T. H. Wilson.** 1980. Substrate specificity and transport properties of the glycerol facilitator of *Escherichia coli*. J. Bacteriol. **144:**274–278.
17. **Herberg, F., S. Bell, and S. Taylor.** 2007. Expression of the catalytic subunit of cAMP-dependent protein kinase in Escherichia coli: multiple isozymes reflect different phosphorylation states. Protein Eng. Design Select. **6:**771–777.
18. **Jokela, J., O. Pastinen, and M. Leisola.** 2002. Isomerization of pentose and hexose sugars by an enzyme reactor packed with cross-linked xylose isomerase crystals. Enzyme Microb. Technol. **31:**67–76.
19. **Jumppanen, J., J. Nurmi, and O. Pastinen.** October 2000. Process for the continuous production of high purity L-ribose. U.S. patent 6,140,498.
20. **Kapust, R., and D. Waugh.** 1999. *Escherichia coli* maltose-binding protein is uncommonly effective at promoting the solubility of polypeptides to which it is fused. Protein Sci. **8:**1668–1674.
21. **Kawaguchi, T., M. Hara, and M. Ueda.** February 2002. Process for producing l-ribose. U.S. patent 6,348,326.
22. **Koeller, K. M., and C. H. Wong.** 2000. Emerging themes in medicinal glycoscience. Nat. Biotechnol. **18:**835–841.
23. **Laemmli, U. K.** 1970. Cleavage of structural proteins during the assembly of the head of bacteriophage T4. Nature **227:**680–685.
24. **Laux, D. C., J. M. Corson, M. Givskov, M. Hentzer, A. Moller, K. A. Wosencroft, J. C. Olson, K. A. Krogfelt, J. B. Goldberg, and P. S. Cohen.** 2002. Lysophosphatidic acid inhibition of the accumulation of *Pseudomonas aeruginosa* PAO1 alginate, pyoverdin, elastase and LasA. Microbiology **148:** 1709–1723.
25. **Lawrence, J. V., and S. Maier.** 1977. Correction for the inherent error in optical density readings. Appl. Environ. Microbiol. **33:**482–484.
26. **Outten, C. E., and T. V. O'Halloran.** 2001. Femtomolar sensitivity of metalloregulatory proteins controlling zinc homeostasis. Science **292:**2488–2492.
27. **Ragupathi, G., F. Koide, P. O. Livingston, Y. S. Cho, A. Endo, Q. Wan, M. K. Spassova, S. J. Keding, J. Allen, O. Ouerfelli, R. M. Wilson, and S. J. Danishefsky.** 2006. Preparation and evaluation of unimolecular pentavalent and hexavalent antigenic constructs targeting prostate and breast cancer: a synthetic route to anticancer vaccine candidates. J. Am. Chem. Soc. **128:** 2715–2725.
28. **Reiner, A. M.** 1975. Genes for ribitol and D-arabitol catabolism in *Escherichia coli*: their loci in C strains and absence in K-12 and B strains. J. Bacteriol. **123:**530–536.
29. **Rouhi, A.** 2004. Chiral chemistry. Chem. Eng. News **82:**47–62.
30. **Sanno, Y., T. H. Wilson, and E. C. Lin.** 1968. Control of permeation to glycerol in cells of *Escherichia coli*. Biochem. Biophys. Res. Commun. **32:** 344–349.
31. **Seo, M., J. An, J. Shim, and G. Kim.** 2003. One-pot inversion of D-mannono-1,4-lactone for the practical synthesis of L-ribose. Tetrahedron Lett. **44:**3051–3052.
32. **Sorensen, H. P., and K. K. Mortensen.** 2005. Advanced genetic strategies for recombinant protein expression in *Escherichia coli*. J. Biotechnol. **115:**113–128.
33. **Stoop, J., W. S. Chilton, and D. M. Pharr.** 1996. Substrate stereospecificity of the NAD-dependent mannitol dehydrogenase from celery. Phytochemistry **43:**1145–1150.
34. **Stoop, J., and D. M. Pharr.** 1993. Effect of different carbon sources on relative growth rate, internal carbohydrates, and mannitol 1-oxidoreductase activity in celery suspension cultures. Plant Physiol. **103:**1001–1008.
35. **Stoop, J., and D. M. Pharr.** 1994. Mannitol metabolism in celery stressed by excess macronutrients. Plant Physiol. **106:**503–511.
36. **Stoop, J., J. D. Williamson, M. A. Conkling, J. J. MacKay, and D. M. Pharr.** 1998. Characterization of NAD-dependent mannitol dehydrogenase from celery as affected by ions, chelators, reducing agents and metabolites. Plant Sci. **131:**43–51.
37. **Stoop, J. M., and D. M. Pharr.** 1992. Partial purification and characterization of mannitol: mannose 1-oxidoreductase from celery (*Apium graveolens* var. *rapaceum*) roots. Arch. Biochem. Biophys. **298:**612–619.
38. **Stoop, J. M., J. D. Williamson, M. A. Conkling, and D. M. Pharr.** 1995. Purification of NAD-dependent mannitol dehydrogenase from celery suspension cultures. Plant Physiol. **108:**1219–1225.
39. **Takahashi, H., Y. Iwai, Y. Hitomi, and S. Ikegami.** 2002. Novel synthesis of L-ribose from D-mannono-1,4-lactone. Organ. Lett. **4:**2401–2403.
40. **Tam, R., D. Averett, and K. Ramasamy.** November 2003. Monocyclic L-nucleosides, analogs and uses thereof. U.S. patent 6,642,206.
41. **Vallee, B., and F. Hoch.** 1955. Zinc, a component of yeast alcohol dehydrogenase. Proc. Natl. Acad. Sci. USA **41:**327–338.
42. **Van, T. D.** April 2003. Process for obtaining bio-functional fractions from biomass. European patent 1,301,542.
43. **Voegele, R. T., G. D. Sweet, and W. Boos.** 1993. Glycerol kinase of *Escherichia coli* is activated by interaction with the glycerol facilitator. J. Bacteriol. **175:**1087–1094.
44. **Williamson, J. D., J. M. Stoop, M. O. Massel, M. A. Conkling, and D. M. Pharr.** 1995. Sequence analysis of a mannitol dehydrogenase cDNA from plants reveals a function for the pathogenesis-related protein ELI3. Proc. Natl. Acad. Sci. USA **92:**7148–7152.